Original Article

Radiomics-clinical nomogram for preoperative tumor-node-metastasis staging prediction in breast cancer patients using dynamic enhanced magnetic resonance imaging

Zhe Yang[1], Shouen Wang[2], Wei Yin[3], Ying Wang[4], Fanghua Liu[1], Jianshu Xu[1], Long Han[1], Chenglong Liu[1]

[1]Department of Radiology, the Second Affiliated Hospital of Shandong First Medical University, Tai'an, China; [2]Department of Pathology, the Second Affiliated Hospital of Shandong First Medical University, Tai'an, China; [3]Department of Radiology, Beijing Friendship Hospital of Capital Medical University, Beijing, China; [4]Department of Radiology, the First Affiliated Hospital of Bengbu Medical University, Bengbu, China

Contributions: (I) Conception and design: Z Yang, C Liu; (II) Administrative support: C Liu, W Yin, Y Wang; (III) Provision of study materials or patients: F Liu, J Xu, L Hu; (IV) Collection and assembly of data: C Liu, Z Yang, F Liu, J Xu, L Han; (V) Data analysis and interpretation: Z Yang, W Yin, S Wang, Y Wang; (VI) Manuscript writing: All authors; (VII) Final approval of manuscript: All authors.

Correspondence to: Chenglong Liu, BM. Department of Radiology, the Second Affiliated Hospital of Shandong First Medical University, 366 Taishan Street, Tai'an 271000, China. Email: liuchenglong12301@163.com.

Background: Breast cancer is one of the most commonly diagnosed malignancies in women worldwide, and the disease burden continues to aggravate. The tumor-node-metastasis (TNM) staging information is crucial for oncology physicians to develop appropriate clinical strategies. This study aimed to investigate the value of a radiomics-clinical model for predicting TNM stage in breast cancer patients using dynamic contrast-enhanced magnetic resonance imaging (DCE-MRI).

Methods: DCE-MRI images from 166 patients with pathologically confirmed breast cancer were retrospectively collected, including early stage (TNM0–TNM2) and locally advanced or advanced stage (TNM3–TNM4). Included patients were divided into a training cohort (n=116) and a test cohort (n=50). The radiomics, clinical and integrated models were constructed and a nomogram was established to distinguish the TNM0–TNM2 stage from the TNM3–TNM4 stage. Receiver operating characteristic (ROC) curves, calibration curves and decision curve analysis (DCA) were employed to assess the predictability of the models.

Results: Eighty-five patients were at the early stages, while 81 patients were at the other stages. In the training and test cohorts, the area under the curve (AUC) values for distinguishing early and advanced breast cancer were 0.870 and 0.818 for the nomogram, respectively. The nomogram calibration curves showed good agreement between the predicted and observed TNM stages in the training and test cohorts. The Hosmer-Lemeshow test showed that the nomogram fit perfectly in the two cohorts. DCA indicated that the nomogram displayed clear superiority in forecasting TNM staging over clinical and radiomic signatures.

Conclusions: Compared to traditional imaging methods, the clinical-radiomics nomogram acquired by DCE-MRI could potentially be utilized to preoperatively evaluate the TNM stage of breast cancer with relatively high accuracy. It can be an effective method to guide clinical decisions.

Keywords: Radiomics; breast cancer; nomogram; tumor-node-metastasis (TNM); magnetic resonance imaging (MRI)

Submitted Sep 02, 2024. Accepted for publication Jan 09, 2025. Published online Mar 18, 2025.
doi: 10.21037/tcr-24-1559
View this article at: https://dx.doi.org/10.21037/tcr-24-1559

Introduction

Breast cancer is one of the most commonly diagnosed malignancies in women worldwide (1). In China, the incidence rate of this cancer has increased in recent decades, with approximately 420,000 new cases and 120,000 deaths in 2020, according to statistics from the National Cancer Center of China. The disease is characterized by a diverse range of conditions with noticeable epidemiological and biological heterogeneity, leading to significantly different disease processes and prognoses (2). Although the breast cancer mortality rate has decreased by 40% in women since 1988 (3), the disease burden continues to aggravate. Accordingly, effectively measurements were highly needed to timely diagnose breast cancer (4).

The tumor-node-metastasis (TNM) staging information is crucial for oncology physicians to develop appropriate clinical strategies. TNM0–2 stages are early cancers, and TNM3 and TNM4 stages are locally advanced and advanced cancers, respectively. The survival rate of patients with stage 3–4 disease is much lower than that of patients with stage 0–2 disease. The 8th edition TNM staging standard for breast cancer was introduced by the American Joint Committee on Cancer (AJCC) in 2016. The latest TNM staging system is more suitable for breast cancer, with the goal of assessing tumors in a clinical setting and offering additional insight to facilitate to optimize treatment methods. Nonetheless, traditional imaging modalities such as magnetic resonance imaging (MRI) and multidetector computed tomography (MDCT) are unable to provide an accurate assessment of TNM stage in patients with breast cancer. Therefore, it is important to develop a more precise method to help to predict the TNM stage in patients with breast cancer.

In 2012, Lambin *et al.* (5) first proposed the concept of radiomics as a non-invasive diagnostic method (6-8) focusing on the high-throughput extraction (9,10) of numerous quantitative imaging features (11-17) related to shape, intensity and texture (18,19) from medical images, offering objective information that is challenging for human eyes to quantify (20). Compared to traditional imaging methods, radiomics can obtain more useful information from images, which can help us understand more characteristics of tumors. Even the features obtained around the tumors, which are usually ignored by previous methods, are also valuable. With great potential, radiomics has been extensively utilized in healthcare for early detection, management, and prognosis prediction (21-26), especially for the diagnosis and treatment of malignant tumors. By utilizing machine learning technology, it is possible to quantitatively evaluate the inherent heterogeneity of tumor lesions and link it to clinical outcomes. There has been a notable surge in the number of studies on breast cancer radiomics. However, to our knowledge, the radiomics studies concerning the TNM staging of breast cancer are rarely seen.

Because TNM stage relies on pathological analysis, it is impossible to evaluate it using traditional imaging methods and clinical data prior to surgery, leading to many difficulties in making proper clinical decisions. In this study, we aimed to preoperatively predict the likelihood of advanced-stage breast cancer. Dynamic contrast-enhanced magnetic resonance imaging (DCE-MRI) was used for image acquisition, and correlation and least absolute shrinkage and selection operator (LASSO) regression analyses were used for feature extraction. Radiomics and clinical models were constructed, and we then developed an integrated model using radiomics and clinical indicators and created a radiomics-clinical nomogram to validate its efficacy. Assuming that the integrated model has good predictive performance, our study would assist clinicians in making proper surgical plans and guiding appropriate clinical interventions. We present this article in accordance with the TRIPOD reporting checklist (available at https://tcr.amegroups.com/article/view/10.21037/tcr-24-1559/rc).

Highlight box

Key findings

- The study integrated radiomics features from dynamic contrast-enhanced magnetic resonance imaging (DCE-MRI) scans with clinical indicators to construct a nomogram for predicting advanced breast cancer probability. The nomogram has excellent performance in differentiating the high and low tumor-node-metastasis (TNM) stages.

What is known and what is new?

- Some indicators, like Ki67, are important predictive factor for TNM staging of breast cancer.
- The clinical factor combined with radiomics features can be a better choice to predict TNM staging for breast cancer.

What is the implication, and what should change now?

- The nomogram offers healthcare professionals a personalized assessment of advanced breast cancer probability before treatment, and further actions are needed to validate its efficacy in wider clinical applications.

Methods

Patient information

The study was conducted in accordance with the Declaration of Helsinki (as revised in 2013). The study was approved by the Ethics Committee of the Second Affiliated Hospital of Shandong First Medical University (2024-012). Due to the retrospective nature of the study, informed consent was waived. Patients with pathologically confirmed breast cancer and receiving DCE-MRI between January 2020 and December 2023 were enrolled. The inclusion criteria were as follows: (I) verification of pathological evidence; (II) image acquisition fitting up with quality control; and (III) full access to all clinical data. The exclusion criteria were as follows: (I) no pathological proof; (II) poor image quality leading to unclear margins of lesions or significant image artifacts affecting visualization; and (III) incomplete clinical results. Patients with missing clinical data were excluded from this study.

Examination

The excised breast tissue was sent for pathological assessment, and a preoperative magnetic resonance scanning was conducted within two weeks before surgery or biopsy. TNM staging was performed based on clinical and radiological data.

A 3.0 T magnetic resonance scanner was used for scanning at the Second Affiliated Hospital of Shandong First Medical University (General Electric Company, Boston, USA). The scanning range included the bilateral breast tissue, anterior chest at the same level, and bilateral armpits. Gadodiamide was injected as a contrast agent through the anterior elbow vein using a double-tube high-pressure injector at a dose of 0.2 mL/kg, and then 20 mL of physiological saline was injected.

The scan parameters for the DCE sequence were as follows: slice thickness, 1.8 mm; slice space, 0.3 mm; field of view (FOV), 360 mm.

TNM staging

The staging of breast cancer was conformed to the 8th Edition of the AJCC Cancer Staging Manual (27). The determination of the T stage depends primarily on the size of the tumor, whereas the assessment of the N stage considers the presence of cancer in regional lymph nodes, and the evaluation of the M stage focuses on the distant metastasis of the cancer.

Image segmentation

Segmentation of breast images in the DCE sequence was performed by two highly experienced radiologists who were unaware of the patients' histopathology results. Radiologist A manually delineated the regions of interest (ROIs) using 3D Slicer 4.11.0, while radiologist B reviewed all segmented ROIs.

The third stage of the dynamic enhancement sequence was selected for delineating the ROI. This particular stage aligns with the medium phase of arterial enhancement in contrast-enhanced MRI scans, showcasing strong lesion enhancement which indicates the level of dysfunctional neovascularization, and facilitating clear visualization of the complete contour of cancerous lesions.

Data preprocessing

We randomly assigned 116 patients to the training cohort and 50 patients to the test cohort at a ratio of 7:3. The predictive model was trained using the entire training dataset, and its performance was evaluated independently using cases from the test dataset. All images were resampled to a standard voxel size of 1 mm × 1 mm × 1 mm to normalize the voxel spacing. Finally, the data were standardized using z score standardization (zero-mean normalization).

Extraction of radiomics feature

There are three groups of handcrafted features: geometry, intensity and texture. The features in the first group describe the characteristics of tumor shape. The features of the second group show the first-order statistical distribution of the voxel intensities inside the tumor. Texture features show the patterns or the second- and high-order spatial distributions of the intensities. The extraction of texture features involves applying multiple techniques, including the methods of the gray-level co-occurrence matrix (GLCM), gray-level run length matrix (GLRLM), gray-level size zone matrix (GLSZM), and neighborhood gray-tone difference matrix (NGTDM).

All feature extractions were completed using the Pyradiomics package in Python version 3.9. To obtain high-throughput features, this study adopted a Laplacian Gaussian filter with sigma values of 2, 3, 4, and 5, and eight wavelet transform algorithms (LLL, LLH, LHL, LHH,

HLL, HLH, HHL, and HHH; L stands for low and H stands for high) were applied to first-order statistical and texture features. We processed these features via z score normalization, resulting in an average feature value of 0 and a standard deviation of 1.

Radiomics feature selection

Correlation

For the features which were highly repeatable, the correlation between them was obtained by Spearman's rank correlation coefficient. The feature with a correlation coefficient less than 0.9 was reserved. A greedy recursive deletion strategy was used to filter features; that is, the feature with the greatest redundancy in the current set is deleted each time. Following the process for selection, a total of 230 features were kept.

LASSO

The LASSO regression model was employed with a discovery dataset to build a signature. By the regulation weight λ, LASSO decreases these regression coefficients toward zero and sets the coefficients of a lot of unrelated features exactly to zero. To get the best λ, we used a 10-fold cross-validation with minimum criteria. The final λ value generated the minimum cross-validation error. The retained features with nonzero coefficients were used for regression model fitting and were integrated into a radiomics model, and then the radiomics score was got for each patient. The formula for this score is indicated in Appendix 1. We used the Python scikit-learn package for LASSO regression modelling. Following this step, eight features were kept in the final model.

Clinical signature

The process used to construct the clinical signature closely resembles that used to construct the rad signature. Clinical features included age, blood pressure, blood sugar, blood fat, human epidermal growth factor receptor 2 (HER2), estrogen receptor (ER), progesterone receptor (PR), and Ki67 [≤14% or >14% defined as low or high expression according to the international expert consensus (28)]. First, the features employed for constructing the clinical signature were chosen based on baseline statistics with $P<0.05$. We have made comparisons among different machine learning models constructed by different machine learning algorithms, like K-Nearest Neighbors (KNN), and Extra-Trees (ET) algorithm was the best one for the final model. The DeLong tests showed that there were significant differences between the models constructed by ET algorithm and other algorithms. So, we selected ET machine learning algorithm to build a risk model. Fivefold cross-validation was used to evaluate this model.

Rad signature

After LASSO feature screening, for the final features, we used the same machine learning (ET) algorithm for the construction of a risk model. Fivefold cross validation was used to get the final signature. Receiver operating characteristic (ROC) curves were drawn to evaluate the performance of this model. Finally, the corresponding area under the curve (AUC), diagnostic accuracy, sensitivity (SEN), specificity (SPE), positive predictive value (PPV), and negative predictive value (NPV) were all analyzed.

Nomogram

By utilizing the analysis for logistic regression, a nomogram was established by integrating the radiomics signature and clinical risk factors to construct an enhanced predictive model. To estimate the accuracy of the TNM staging based on the nomogram, a calibration curve was generated for comparison with actual observation data. We employed decision curve analysis (DCA) to evaluate these models.

Statistical analysis

Statistical analysis was conducted by using the Python Stata models (version 0.13.2) package. We considered a P value <0.05 as statistically significant. For continuous variables, we used student's *t*-test or Mann-Whitney *U* test for comparison, and we made the comparison of categorical variables using the chi-square test or Fisher's exact test.

Results

Patient characteristics

One hundred and sixty-six of the 212 patients were included in this study (*Figure 1A*), including 165 female patients and 1 male patient. The distribution of these cases is shown in *Table 1*. With more than 160 cases, we thought this sample size was relatively large to decrease the bias owing to a small sample size, and a large number of literatures have used similar number of the sample size to get satisfactory results, further proving the reliability of this sample size

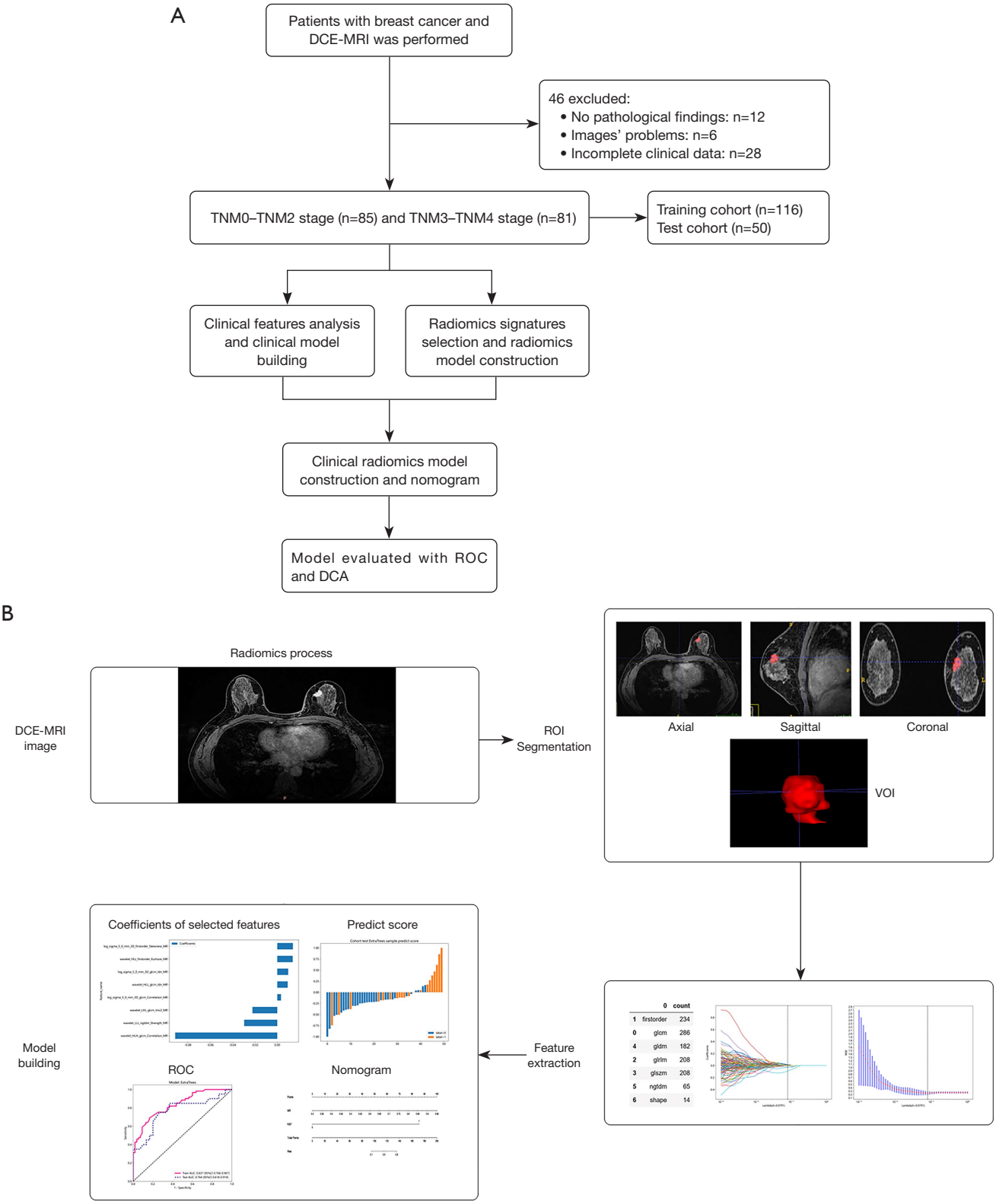

Figure 1 Two flow charts. (A) The flow chart of this study; (B) the radiomics process flow chart. AUC, area under the curve; CI, confidence interval; DCA, decision curve analysis; DCE-MRI, dynamic contrast-enhanced magnetic resonance imaging; GLCM, gray-level co-

occurrence matrix; GLDM, gray level dependence matrix; GLRLM, gray-level run length matrix; GLSZM, gray-level size zone matrix; HLH, high-low-high; HLL, high-low-low; LHL, low-high-low; LLL, low-low-low; MR, magnetic resonance; MSE, mean standard errors; NGTDM, neighborhood gray-tone difference matrix; ROI, region of interest; ROC, receiver operating characteristic; TNM, tumor-node-metastasis; VOI, volume of interest.

Table 1 Baseline characteristics of patients in cohorts

Feature name	Train				Test			
	All	TNM0–2 (n=55)	TNM3–4 (n=61)	P value	All	TNM0–2 (n=30)	TNM3–4 (n=20)	P value
Age (years)	52.75±12.13	51.62±10.92	53.77±13.13	0.34	48.82±11.10	48.07±11.10	49.95±11.29	0.56
Blood pressure				0.46				>0.99
–	86 (74.14)	43 (78.18)	43 (70.49)		44 (88.00)	26 (86.67)	18 (90.00)	
+	30 (25.86)	12 (21.82)	18 (29.51)		6 (12.00)	4 (13.33)	2 (10.00)	
Blood sugar				0.13				0.28
–	91 (78.45)	47 (85.45)	44 (72.13)		40 (80.00)	22 (73.33)	18 (90.00)	
+	25 (21.55)	8 (14.55)	17 (27.87)		10 (20.00)	8 (26.67)	2 (10.00)	
Blood fat				0.17				0.67
–	34 (29.31)	20 (36.36)	14 (22.95)		18 (36.00)	12 (40.00)	6 (30.00)	
+	82 (70.69)	35 (63.64)	47 (77.05)		32 (64.00)	18 (60.00)	14 (70.00)	
HER2				0.050				0.72
–	96 (82.76)	50 (90.91)	46 (75.41)		41 (82.00)	24 (80.00)	17 (85.00)	
+	20 (17.24)	5 (9.09)	15 (24.59)		9 (18.00)	6 (20.00)	3 (15.00)	
ER				0.36				>0.99
–	22 (18.97)	8 (14.55)	14 (22.95)		6 (12.00)	4 (13.33)	2 (10.00)	
+	94 (81.03)	47 (85.45)	47 (77.05)		44 (88.00)	26 (86.67)	18 (90.00)	
PR				0.46				0.58
_	30 (25.86)	12 (21.82)	18 (29.51)		8 (16.00)	6 (20.00)	2 (10.00)	
+	86 (74.14)	43 (78.18)	43 (70.49)		42 (84.00)	24 (80.00)	18 (90.00)	
Ki67				<0.001				0.056
≤14%	13 (11.21)	13 (23.64)	0		7 (14.00)	7 (23.33)	0	
>14%	103 (88.79)	42 (76.36)	61 (100.00)		43 (86.00)	23 (76.67)	20 (100.00)	

"–" represents negative; "+" represents positive. The numbers in the row of age were shown as mean ± SD, and numbers in other rows were shown as number (percent). ER, estrogen receptor; HER2, human epidermal growth factor receptor 2; PR, progesterone receptor; SD, standard deviation; TNM, tumor-node-metastasis.

and indicating that the sample size was appropriate for our study. Furthermore, we have used Synthetic Minority Over-Sampling Technique (SMOTE) to effectively improved the imbalance of the data distribution, with good ability to avoid overfitting. This sample size ensured a relatively high accuracy of the statistical analysis, preventing possible bias due to the unbalanced distribution of cases.

All the patients underwent surgical intervention or biopsy. The average age of the 166 patients was 51.57±11.94 years (aged 25–78 years), with 50.36±11.05 years in the early stages and 52.83±12.74 years in the advanced stages. A pathologist blindly reviewed the pathological data. In the

Table 2 Simple and multiple regression analysis in train cohort

Feature name	Single factor				Multiple factor			
	OR	Lower 95% CI	Upper 95% CI	P value	OR	Lower 95% CI	Upper 95% CI	P value
ER	0.872	0.717	1.062	0.25	–	–	–	–
PR	0.905	0.759	1.079	0.35	–	–	–	–
Age	1.004	0.997	1.010	0.34	–	–	–	–
Blood pressure	1.105	0.927	1.318	0.35	–	–	–	–
Blood fat	1.175	0.993	1.391	0.12	–	–	–	–
Blood sugar	1.217	1.010	1.467	0.08	–	–	–	–
HER2	1.311	1.073	1.603	0.03	1.216	1.004	1.473	0.09
Ki67	1.808	1.439	2.270	<0.001	1.741	1.384	2.188	<0.001

CI, confidence interval; ER, estrogen receptor; HER2, human epidermal growth factor receptor 2; OR, odds ratio; PR, progesterone receptor.

training cohort, there were 55 patients with early-stage breast cancer (33.1%) and 61 patients with advanced cancer (36.7%), while in the test cohort, there were 30 patients with early-stage breast cancer (18.1%) and 20 patients with advanced cancer (12.0%). The clinical characteristics of the patients for both the training and testing sets were provided in *Table 1*. These characteristics all showed no significant differences between the training and testing sets (P>0.05). *Table 2* shows the results of the simple and multiple regressions for the patients' baseline characteristics, indicating that Ki67 expression was significantly different in the training cohort.

Feature selection and construction of radiomics signature

Features statistics: we extracted 1,197 handcrafted features, consisting of 234 first-order features, 14 shape features, and 949 texture features, using an in-house feature analysis program by Pyradiomics.

LASSO feature selection: nonzero coefficients were used to establish the Rad-score using a LASSO logistic regression model. The coefficients and mean standard errors (MSEs) of these radiomics features are visually represented in *Figure 1B*.

The correct classification rate of TNM stage cases in the two cohorts was illustrated by two confusion matrix maps (Figure S1). The prediction scores in these cohorts for each patient are shown in *Figure 2*.

The model was obtained by using radiomics features with an ET classifier.

Clinical signature development

Analysis of differences between different TNM stages revealed that Ki67 expression was an independent clinical risk factor for TNM stage (*Table 2*). The clinical signature was composed of this factor. *Table 3* shows the performance of this clinical signature.

Combined models and radiomics-clinical nomogram

The integration of the radiomics and clinical signatures led to the set-up of a unified model. The performance of the integrated model was excellent in both the training cohort (AUC =0.870) and the test cohort (AUC =0.818) (*Table 3*, *Figure 3A*,*3B*). The performance metrics of these models, including the diagnostic accuracy, SEN, SPE, PPV, and NPV, are presented in *Table 3*. Additionally, a nomogram was established. The nomogram allows for the accumulation of points for each variable onto the relevant axis to determine the risk of advanced TNM staging. Increased scores indicate an elevated likelihood of advanced TNM stages in cancer patients. We chose the DeLong test for the comparison of the AUC values of different models. These models all demonstrated significant differences in the two cohorts.

The calibration curves for the nomogram showed good consistency between the predicted and observed results of TNM stages in the two cohorts. The P values of the Hosmer-Lemeshow test were calculated for these models. The nomogram performed well in both the training

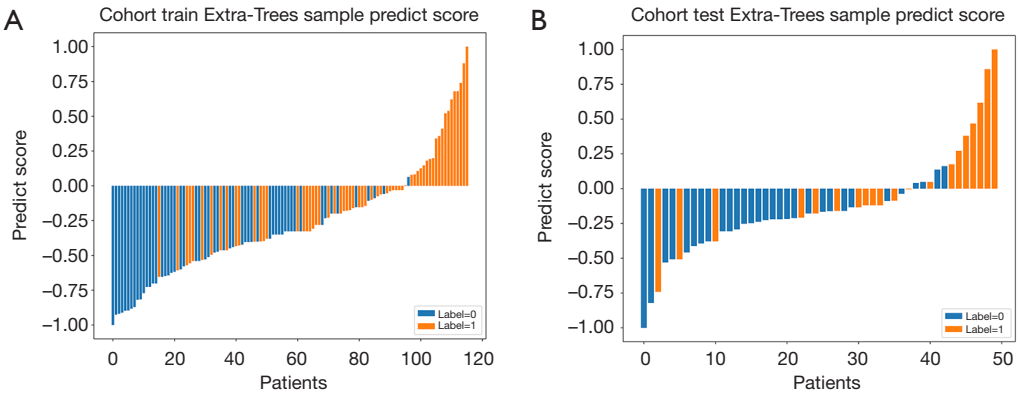

Figure 2 Comparison between different cohorts. Extra-Trees sample prediction score in the training (A) and test (B) cohorts. Each number of the X-axis represents one patient, and numbers in the Y-axis represents the predict score values. The blue columns represent patients in the TNM 0–2 group, and the orange columns represent patients in the TNM 3–4 group. TNM, tumor-node-metastasis.

Table 3 Comparison of parameters of various models

Signature	Accuracy	AUC (95% CI)	Sensitivity	Specificity	PPV	NPV	Threshold
Training cohort							
Clinic	0.474	0.618 (0.5615–0.6748)	0.000	1.000	0.000	0.474	0.592
MR	0.750	0.837 (0.7663–0.9068)	0.672	0.836	0.820	0.697	0.516
Nomogram	0.759	0.870 (0.8092–0.9312)	0.672	0.855	0.837	0.701	0.564
Test cohort							
Clinic	0.600	0.617 (0.5397–0.6936)	0.000	1.000	0.000	0.600	0.592
MR	0.740	0.764 (0.6182–0.9101)	0.700	0.767	0.667	0.793	0.510
Nomogram	0.760	0.818 (0.6970–0.9397)	0.800	0.733	0.667	0.846	0.550

The clinic, MR and nomogram in the first three rows were the models in the training cohort and in the last three rows were in the test cohort. AUC, area under the curve; CI, confidence interval; MR, magnetic resonance; NPV, negative predictive value; PPV, positive predictive value.

(P=0.51) and test cohorts (P=0.54). *Figure 3C,3D* shows the calibration curves for the two different cohorts.

In our study, we evaluated these models by using DCA. The DCA results for the clinical signature, radiomics signature and radiomics-clinical nomogram are shown in *Figure 3E,3F*. The significance of radiomics features was shown in *Figure 4*. In comparison to the baselines, the clinical-radiomic nomogram significantly improved the results with a prediction probability of 0.12–0.78 better than the clinical signature (0.00–0.59) and radiomic signature (0.31–0.90) in the training cohort. The nomogram displayed clear superiority in forecasting TNM staging over clinical and radiomic signatures, suggesting that utilizing a radiomics-clinical nomogram in preoperative TNM staging prediction yields greater advantages.

Discussion

In the present study, a nomogram model was established based on the radiomics and clinical signatures. The integrated approach showed great potential to improve the accuracy of predicting the TNM stage of breast cancer patients. Therefore, this approach might be regarded as the alternative strategy for diagnosing and staging of breast cancer. The elevated levels of SPE in the preoperative identification of unresected lesions emphasize the importance of radiomics as a valuable tool in making precise and personalized regimen for each breast cancer.

A predictive model utilizing the ET algorithm was trained on radiomic features extracted from the DCE-MRI sequence, achieving an AUC of 0.84, SEN of 0.67

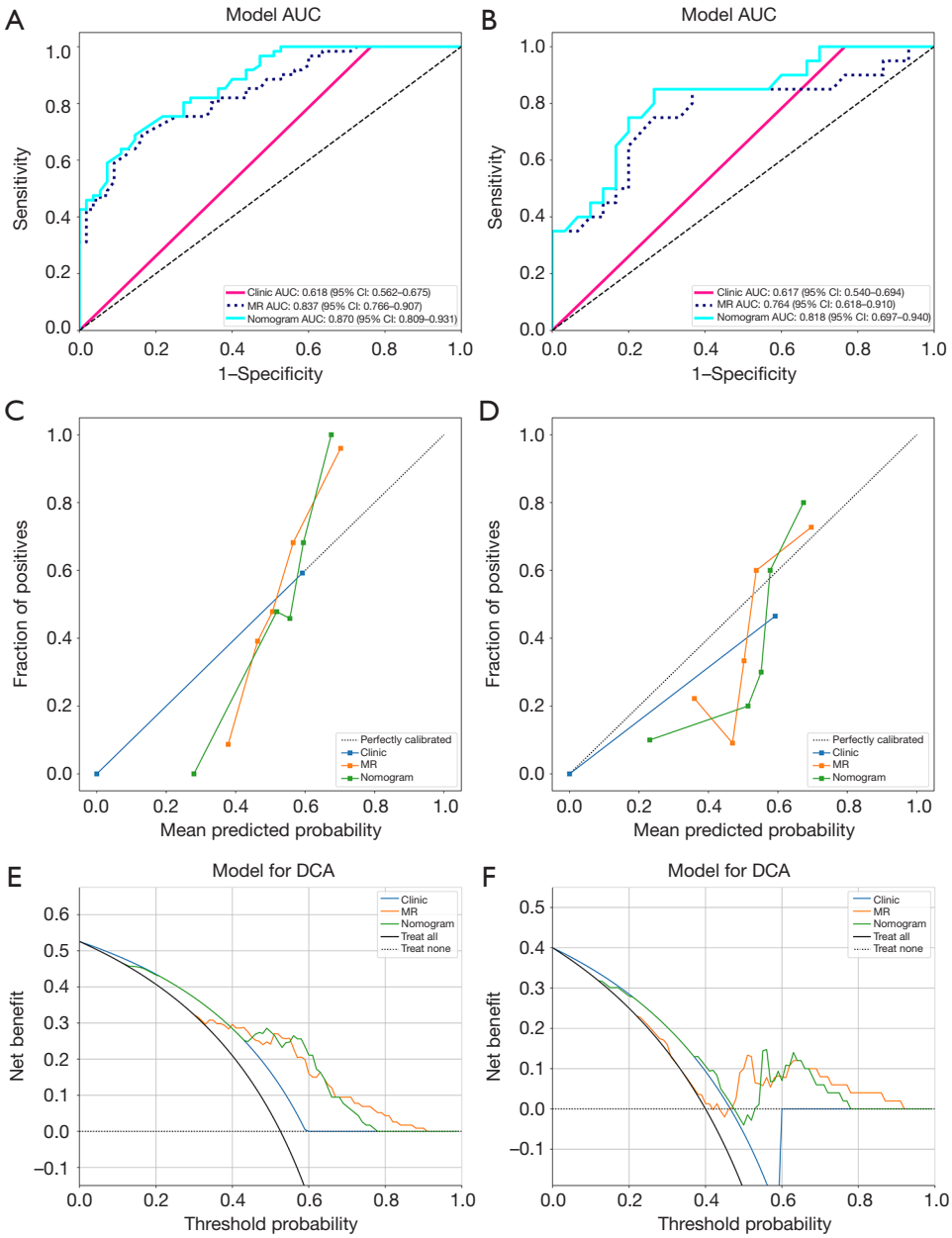

Figure 3 Several curves of the models. (A,B) The AUCs in the training and test cohorts. (C,D) The calibration curves in training and test cohorts. (E,F) The decision curves in the training and test cohorts. AUC, area under the curve; DCA, decision curve analysis; MR, magnetic resonance.

and SPE of 0.84 in the training cohort. Combined with the clinic model using Ki67 indicator, the AUC value of nomogram reached 0.87. Currently, we have not found any studies using machine learning algorithm to predict the TNM stages of breast cancer. However, many previous studies (29,30) have focused on the TNM staging of other tumors using machine learning algorithm. Wu *et al.* (31) reported a clinical-radiomics model for pancreatic ductal adenocarcinoma with satisfactory diagnostic efficacy to differentiate the early TNM stages from advanced stages, achieving an AUC of 0.97, SEN of 0.93, SPE of 0.91, slightly higher than our study. They used tumour diameter and normalized iodine density (ID) value at the portal venous phase (NID-PVP) to construct the clinical model,

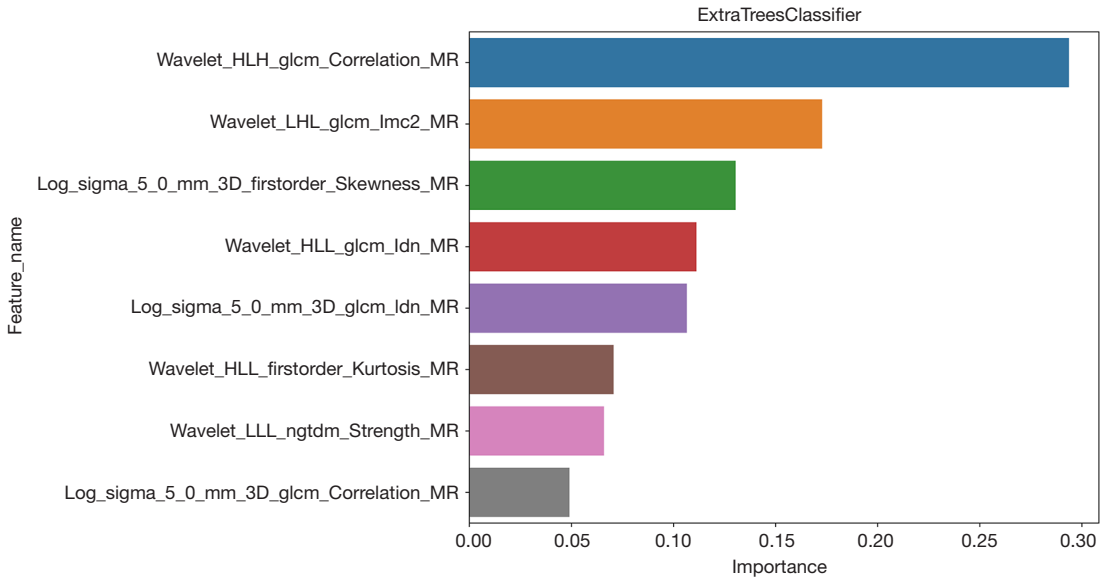

Figure 4 The significance of radiomics features. GLCM, gray-level co-occurrence matrix; HLH, high-low-high; HLL, high-low-low; LHL, low-high-low; LLL, low-low-low; MR, magnetic resonance; NGTDM, neighborhood gray-tone difference matrix.

and two different radiomics models were built by different kinds of radiomics features from polyenergetic and 40-keV virtual monoenergetic images of spectral detector computed tomography (CT), different from our study. Compared to our study, they used more shape and less first-order features to construct radiomics models. Our research highlighted the use of machine learning classifiers trained on MRI-based radiomics for the prediction of TNM stage in patients with breast cancer. By incorporating random features and thresholds for node splitting, ET, as an ensemble learning technique, provides extra randomness and control overfitting and variance, although this trade-off can potentially increase bias in the model. In contrast to various machine learning classifiers, such as random forests, it typically exhibits swiftness during training.

Multiple imaging modalities have been utilized in the diagnosis of breast cancer. Nevertheless, CT and mammography are ineffective in detecting small breast lesions, which are frequently iso-dense. By offering enhanced soft tissue resolution, MRI enables operators to visually increase the detection rate. By utilizing DCE-MRI, the detection of suspected lesions is enhanced, allowing for a rough assessment of their malignancy risk based on patterns observed in enhancement-type curves. Pan *et al.* (32) reported that the coincidence rate of breast cancer detection via MRI was significantly greater than that via ultrasound (US), with SEN, SPE, NPV, PPV and Youden index (YI) values of 89.29%, 63.75%, 81.17%, 77.27%, and 53.04, respectively. Proper evaluation of metastatic lymph nodes plays a pivotal role in classifying the TNM stage. de Felice C *et al.* (33) found that MRI is a reliable technique for examining the layout of axillary lymph nodes prior to surgery and shows promise as a standard procedure for assessing metastatic lymph nodes before undergoing axillary lymph node dissection (ALND). Considering the presence of positive and borderline metastatic lymph nodes, an SEN of 75.7%, an SPE of 99.3%, a PPV of 96.1%, and an NPV of 95% were achieved. Nevertheless, MRI remains an inadequate substitute for histological examination, particularly for accurately assessing the TNM stage.

Radiomics is a rapidly growing area of research in the groundbreaking realm of personalized healthcare. In recent years, great progression of radiomics has been witnessed in the field of oncology imaging. Several radiomics models have been created for predicting the prognosis of clinical interventions across various malignant neoplasms, and references (34-39) have shown tremendous potential over conventional imaging methods. Radiomics analysis may offer a standardized and precise diagnostic method and can also function as a supplemental clinical tool that provides valuable insights into medical decision-making. At present, it has been applied to the prediction of low and high TNM

stages for many tumors, including clear cell renal cell carcinoma (40), with the highest AUC value reaching 0.80 (95% confidence interval: 0.74–0.86).

Despite the potential of radiomics for diagnostic, prognostic, and predictive purposes, this method continues to confront with great challenges. The lack of consistency in radiomics research frequently leads to unreliable results, mainly owing to retrospective design of many related studies. Accordingly, there still lack of standardized agreement in imaging protocols such as acquisition and reconstruction parameters. Research has demonstrated that utilizing automatic image segmentation can significantly enhance the consistency of texture features, making it the recommended approach for increasing the standardization of radiomics analyses. In addition, insufficient validation coupled with the occurrence of type I statistical errors hinders the adoption of new practices in clinical settings. Moreover, the reproducibility of radiomic features could also be influenced by variations in imaging modalities or scanners used, making the radiomics results potentially less generalizable to diverse disease entities.

In our study, we incorporated the Ki67 protein expression marker to design a clinical model that integrated a radiomics model to improve predictive accuracy. Ki67 continues to be a key indicator for predicting the growth, recurrence, and metastasis of breast cancer. The progression of it significantly influences the progression to a higher TNM stage before surgery. Ki67 immunohistochemistry (IHC) is more sensitive to fixation variability than ER or HER2 markers (41). Multiple studies (42,43) have indicated that Ki67 is valuable for predicting prognosis, determining adjuvant treatment options, and predicting response to neoadjuvant treatment in patients with $ER^+/HER2^-$ breast cancer (44). Similarly, Ki67 played an important role in our comprehensive model.

Limitations

Our study has several limitations. This study is of retrospective design, and prospective validation is necessary in future to confirm the value of radiomics in diagnosing and staging of breast cancer, and multiple-center are needed to verify these results. Moreover, we exclusively employed DCE-MRI scans to conduct the radiomics analysis, resulting in minimized fluctuations in the acquisition settings. To optimize future performance, it is imperative to incorporate a variety of imaging sequences, including diffusion-weighted and T2-weighted imaging, into our model.

Conclusions

In conclusion, our findings preliminarily suggest that the clinical-radiomics nomogram acquired by DCE-MRI could potentially be utilized to evaluate the TNM stage of breast cancer preoperatively with relatively high accuracy. Moreover, the nomogram combining radiomics and clinical factors may facilitate making a personalized assessment of advanced breast cancer probability, which shows great potential to help make clinical strategies.

Acknowledgments

We would like to thank the Imaging Department of the Second Affiliated Hospital of Shandong First Medical University for ongoing support.

Footnote

Reporting Checklist: The authors have completed the TRIPOD reporting checklist. Available at https://tcr.amegroups.com/article/view/10.21037/tcr-24-1559/rc

Data Sharing Statement: Available at https://tcr.amegroups.com/article/view/10.21037/tcr-24-1559/dss

Peer Review File: Available at https://tcr.amegroups.com/article/view/10.21037/tcr-24-1559/prf

Funding: This study was supported by grants from Shandong Medical and Health Science Technology Development Program (No. 202309010656), Tai'an City Science and Technology Development Plan (No. 2022NS305), and Shandong School Health Association Science Project (No. SDWS2023063).

Conflicts of Interest: All authors have completed the ICMJE uniform disclosure form (available at https://tcr.amegroups.com/article/view/10.21037/tcr-24-1559/coif). All authors report that this study was supported by grants from Shandong Medical and Health Science Technology Development Program (No. 202309010656), Tai'an City Science and Technology Development Plan (No. 2022NS305), and Shandong School Health Association Science Project (No. SDWS2023063). The authors have no other conflicts of interest to declare.

Ethical Statement: The authors are accountable for all aspects of the work in ensuring that questions related

to the accuracy or integrity of any part of the work are appropriately investigated and resolved. The study was conducted in accordance with the Declaration of Helsinki (as revised in 2013). The study was approved by the Ethics Committee of the Second Affiliated Hospital of Shandong First Medical University (2024-012). Due to the retrospective nature of the study, informed consent was waived.

References

1. Brem RF, Lenihan MJ, Lieberman J, et al. Screening breast ultrasound: past, present, and future. AJR Am J Roentgenol 2015;204:234-40.
2. Díaz-Gavela AA, Del Cerro Peñalver E, Sanchez García S, et al. Breast cancer radiotherapy: What physicians need to know in the era of the precision medicine. Breast Dis 2021;40:1-16.
3. Grabinski VF, Brawley OW. Disparities in Breast Cancer. Obstet Gynecol Clin North Am 2022;49:149-65.
4. Tao Z, Shi A, Lu C, et al. Breast Cancer: Epidemiology and Etiology. Cell Biochem Biophys 2015;72:333-8.
5. Lambin P, Rios-Velazquez E, Leijenaar R, et al. Radiomics: extracting more information from medical images using advanced feature analysis. Eur J Cancer 2012;48:441-6.
6. Luo Y, Sun X, Kong X, et al. A DWI-based radiomics-clinical machine learning model to preoperatively predict the futile recanalization after endovascular treatment of acute basilar artery occlusion patients. Eur J Radiol 2023;161:110731.
7. Bogowicz M, Vuong D, Huellner MW, et al. CT radiomics and PET radiomics: ready for clinical implementation? Q J Nucl Med Mol Imaging 2019;63:355-70.
8. Chen X, Yu Q, Peng J, et al. A Combined Model Integrating Radiomics and Deep Learning Based on Contrast-Enhanced CT for Preoperative Staging of Laryngeal Carcinoma. Acad Radiol 2023;30:3022-31.
9. Zhou Y, Zheng X, Sun Z, et al. Analysis of Bladder Cancer Staging Prediction Using Deep Residual Neural Network, Radiomics, and RNA-Seq from High-Definition CT Images. Genet Res (Camb) 2024;2024:4285171.
10. Li Y, Yang L, Gu X, et al. Computed tomography radiomics identification of T1-2 and T3-4 stages of esophageal squamous cell carcinoma: two-dimensional or three-dimensional? Abdom Radiol (NY) 2024;49:288-300.
11. Liu Z, Wang S, Dong D, et al. The Applications of Radiomics in Precision Diagnosis and Treatment of Oncology: Opportunities and Challenges. Theranostics 2019;9:1303-22.
12. Jang K, Russo C, Di Ieva A. Radiomics in gliomas: clinical implications of computational modeling and fractal-based analysis. Neuroradiology 2020;62:771-90.
13. Chaddad A, Kucharczyk MJ, Daniel P, et al. Radiomics in Glioblastoma: Current Status and Challenges Facing Clinical Implementation. Front Oncol 2019;9:374.
14. Huang EP, O'Connor JPB, McShane LM, et al. Criteria for the translation of radiomics into clinically useful tests. Nat Rev Clin Oncol 2023;20:69-82.
15. Berbís MÁ, Godino FP, Rodríguez-Comas J, et al. Radiomics in CT and MR imaging of the liver and pancreas: tools with potential for clinical application. Abdom Radiol (NY) 2024;49:322-40.
16. Wu S, Wei Y, Li H, et al. A Predictive Clinical-Radiomics Nomogram for Differentiating Tuberculous Spondylitis from Pyogenic Spondylitis Using CT and Clinical Risk Factors. Infect Drug Resist 2022;15:7327-38.
17. Tang FH, Fong YW, Yung SH, et al. Radiomics-Clinical AI Model with Probability Weighted Strategy for Prognosis Prediction in Non-Small Cell Lung Cancer. Biomedicines 2023;11:2093.
18. Martin P, Holloway L, Metcalfe P, et al. Challenges in Glioblastoma Radiomics and the Path to Clinical Implementation. Cancers (Basel) 2022;14:3897.
19. Xiong S, Fu Z, Deng Z, et al. Machine learning-based CT radiomics enhances bladder cancer staging predictions: A comparative study of clinical, radiomics, and combined models. Med Phys 2024;51:5965-77.
20. Chee CG, Yoon MA, Kim KW, et al. Combined radiomics-clinical model to predict malignancy of vertebral compression fractures on CT. Eur Radiol 2021;31:6825-34.
21. Napel S, Mu W, Jardim-Perassi BV, et al. Quantitative imaging of cancer in the postgenomic era: Radio(geno)mics, deep learning, and habitats. Cancer 2018;124:4633-49.
22. Yu Y, He Z, Ouyang J, et al. Magnetic resonance imaging

radiomics predicts preoperative axillary lymph node metastasis to support surgical decisions and is associated with tumor microenvironment in invasive breast cancer: A machine learning, multicenter study. EBioMedicine 2021;69:103460.
23. Wang X, Xie T, Luo J, et al. Radiomics predicts the prognosis of patients with locally advanced breast cancer by reflecting the heterogeneity of tumor cells and the tumor microenvironment. Breast Cancer Res 2022;24:20.
24. Liu C, Zhao W, Xie J, et al. Development and validation of a radiomics-based nomogram for predicting a major pathological response to neoadjuvant immunochemotherapy for patients with potentially resectable non-small cell lung cancer. Front Immunol 2023;14:1115291.
25. Neri E, Del Re M, Paiar F, et al. Radiomics and liquid biopsy in oncology: the holons of systems medicine. Insights Imaging 2018;9:915-24.
26. Gangil T, Sharan K, Rao BD, et al. Utility of adding Radiomics to clinical features in predicting the outcomes of radiotherapy for head and neck cancer using machine learning. PLoS One 2022;17:e0277168.
27. Edition S, Edge S, Byrd D. AJCC cancer staging manual. American Joint Committee on Cancer; 2017.
28. Goldhirsch A, Wood WC, Coates AS, et al. Strategies for subtypes--dealing with the diversity of breast cancer: highlights of the St. Gallen International Expert Consensus on the Primary Therapy of Early Breast Cancer 2011. Ann Oncol 2011;22:1736-47.
29. Blüthgen C, Patella M, Euler A, et al. Computed tomography radiomics for the prediction of thymic epithelial tumor histology, TNM stage and myasthenia gravis. PLoS One 2021;16:e0261401.
30. Liu S, Liang W, Huang P, et al. Multi-modal analysis for accurate prediction of preoperative stage and indications of optimal treatment in gastric cancer. Radiol Med 2023;128:509-19.
31. Wu L, Cen C, Yue X, et al. A clinical-radiomics nomogram based on dual-layer spectral detector CT to predict cancer stage in pancreatic ductal adenocarcinoma. Cancer Imaging 2024;24:55.
32. Pan Q, Ji J. Diagnostic value of ultrasound combined with magnetic resonance imaging in different stages of breast cancer. Oncol Lett 2019;17:209-14.
33. de Felice C, Cipolla V, Stagnitti A, et al. Diagnostic accuracy of 1.5 Tesla breast magnetic resonance imaging in the pre-operative assessment of axillary lymph nodes. Eur J Gynaecol Oncol 2015;36:447-51.
34. Guo L, Du S, Gao S, et al. Delta-Radiomics Based on Dynamic Contrast-Enhanced MRI Predicts Pathologic Complete Response in Breast Cancer Patients Treated with Neoadjuvant Chemotherapy. Cancers (Basel) 2022;14:3515.
35. Bitencourt AGV, Gibbs P, Rossi Saccarelli C, et al. MRI-based machine learning radiomics can predict HER2 expression level and pathologic response after neoadjuvant therapy in HER2 overexpressing breast cancer. EBioMedicine 2020;61:103042.
36. Xia X, Li D, Du W, et al. Radiomics Based on Nomogram Predict Pelvic Lymphnode Metastasis in Early-Stage Cervical Cancer. Diagnostics (Basel) 2022;12:2446.
37. Du G, Zeng Y, Chen D, et al. Application of radiomics in precision prediction of diagnosis and treatment of gastric cancer. Jpn J Radiol 2023;41:245-57.
38. Qu J, Ma L, Lu Y, et al. DCE-MRI radiomics nomogram can predict response to neoadjuvant chemotherapy in esophageal cancer. Discov Oncol 2022;13:3.
39. Wang L, Wu X, Tian R, et al. MRI-based pre-Radiomics and delta-Radiomics models accurately predict the post-treatment response of rectal adenocarcinoma to neoadjuvant chemoradiotherapy. Front Oncol 2023;13:1133008.
40. Demirjian NL, Varghese BA, Cen SY, et al. CT-based radiomics stratification of tumor grade and TNM stage of clear cell renal cell carcinoma. Eur Radiol 2022;32:2552-63.
41. Nielsen TO, Leung SCY, Rimm DL, et al. Assessment of Ki67 in Breast Cancer: Updated Recommendations From the International Ki67 in Breast Cancer Working Group. J Natl Cancer Inst 2021;113:808-19.
42. Lalkota BP, Srinivasa BJ, Swamy MV, et al. The role of p53 and ki67 in predicting clinical outcome in breast cancer patients. J Cancer Res Ther 2023;19:208-13.
43. Chidananda Murthy G. Ki-67 Index and Its Correlation with Clinical and Pathological Variables in Breast Cancer. Indian J Surg Oncol 2023;14:943-8.
44. Penault-Llorca F, Radosevic-Robin N. Ki67 assessment in breast cancer: an update. Pathology 2017;49:166-71.

Cite this article as: Yang Z, Wang S, Yin W, Wang Y, Liu F, Xu J, Han L, Liu C. Radiomics-clinical nomogram for preoperative tumor-node-metastasis staging prediction in breast cancer patients using dynamic enhanced magnetic resonance imaging. Transl Cancer Res 2025;14(3):1836-1848. doi: 10.21037/tcr-24-1559